COSTA RICA INSTITUTE OF TECHNOLOGY

SCHOOL OF BIOLOGY

BIOTECHNOLOGY ENGINEERING

FINAL GRADUATION PROJECT

VALIDATION OF SUCCINATION TARGETS AND ITS EFFECTS ON *ESCHERICHIA COLI*

Institut Pasteur

María José Navarro Porras

Cartago, April 2022.

VALIDATION OF SUCCINATION TARGETS AND ITS EFFECTS ON *ESCHERICHIA COLI*

María José Navarro Porras

ABSTRACT

Succination is a non-enzymatic and covalent PTM of cysteine by the TCA cycle metabolite fumarate, which results in the formation of S-(2-succino)cysteine (2SC), a mitochondrial stress indicator. It causes wide-ranging effects on eukaryotic metabolism, but has not been well-established for prokaryotic organisms. Therefore, the aim of this project is to validate in *E. coli* some succination targets previously revealed by proteomics, of which some are proteins with Fe-S clusters. The experiments were elaborated according to two methodologies, using Dimethyl Fumarate (DMF), its active compound Monomethyl-Fumarate (MMF), and fumarase depletion Δ*fumABC* mutant to drive fumarate accumulation. It was demonstrated that supplementation with glutamine, adenine and xanthine (GAX) was able to overcome the toxic effect of DMF on the mutants at sub-MIC of the drug. Also, a Δ*fumABC* mutant manages to recover a growth rate similar to the WT strain when supplemented with GAX. For the second part, enzymatic assays were performed to measure the specific activity of fumarase and aconitase. The Fe-S proteins decreased their enzymatic activity when exposed to DMF and fumarase depletion treatments. Among all, Fe-S clusters appear to have a protecting role from succination on their coordinating cysteines. The results obtained contribute to the evidence that succination is a significant PTM and a potential key mechanism linking multiple pathways that may cause dysregulation of cell metabolism in prokaryotes.

Keywords: Fe-S clusters, TCA cycle, fumarate, enzymology, metabolism perturbation.

- FINAL GRADUATION PROJECT REPORT. Ingeniería en Biotecnología. Escuela de Biología. Instituto Tecnológico de Costa Rica, Cartago, Costa Rica. 2022.

VALIDATION OF SUCCINATION TARGETS AND ITS EFFECTS ON *ESCHERICHIA COLI*

Report submitted to the School of Biology of the Costa Rican Institute of Technology as a partial requirement to opt for the bachelor's degree in Biotechnology Engineering.

Tribunal members

_____

M.Sc. Luis Barboza Fallas.

ITCR Tutor.

_____   _____
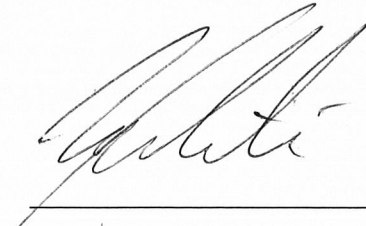
PhD. Rodrigo Arias Cartín.   PhD. Erick Hernández Carvajal.

Institution Tutor.   **ITCR Lector.**

DEDICATION

To my father, my sister and my dog, for being my main support.

To my family and friends who have always helped me.

To all the people and events that made my dream possible.

ACKNOWLEDGEMENTS

INDEX

TABLE INDEX

FIGURES INDEX

INTRODUCTION

Escherichia coli, among the Enterobacteriaceae family, is the most used model organism due to its ability to grow fast using diverse substrates and be genetically manipulated (Adamczyk *et al*., 2017). As a fairly typical gram-negative bacillus, its metabolic plasticity gives to *E. coli* a remarkable ecological ubiquity, as it can quickly adapt and bloom in various environments (Blount, 2015). However, the exposure to those different external conditions may impact its cell cycle, growth rate and morphology, and trigger several physiological strategies to survive, such as stress responses and changes in principal cell pathways (central carbon metabolism (CCM), DNA and cell wall synthesis, etc.) (Westfall & Levin, 2018). Therefore, it is of great importance to study how some conditions impact bacterial cell growth and metabolism (Hug & Gaut, 2015).

The CCM is a series of enzymatic reactions that convert sugars into energy and precursors for the entire biomass of the cell. The tricarboxylic acid (TCA) cycle, also known as citric acid cycle or Krebs cycle, is a universal CCM pathway which fuels energy and some metabolites from the oxidation of acetyl-CoA derived from aminoacids, fatty acids and carbohydrates (Jung & Mack, 2018). The intracellular excess of some TCA intermediates may alter the cell. For example, it was recently discovered that accumulated fumarate can react covalently with thiol groups on cysteine residues to generate the stable adduct S-(2-succinyl)cysteine (2SC) (Ruecker *et al*., 2017). This process, also termed as succination, leads to physiological consequences such as decreasing functionality to complete inactivation of target proteins (Piroli *et al*., 2016).

The succination process appears to be specific and irreversible for cysteine, as previous studies have been unable to detect succination of other candidate nucleophilic amino acids and no salvage mechanism is known to rescue succinated cysteines in the cell (Merkley *et al*., 2014; Jové *et al*., 2020). Despite cysteine being one of the least common amino acids in proteins (Merkley *et al*., 2014), it is essential, since it often

plays a major role in the active site of proteins and in the coordination of metal cofactors (Blanc *et al*., 2015). Notably, the L-cysteine provides the sulfur atom for Iron Sulfur (Fe-S) clusters assembly and the cysteine residues coordinate the iron within proteins (Tsaousis, 2019). Fe-S clusters are simple inorganic protein cofactors composed of ferrous ($Fe2+$) or ferric ($Fe3+$) iron and sulfide ($S2-$) ions (Braymer *et al*., 2021). There are involved in a variety of cellular processes such as DNA replication, DNA repair, transcription regulation, RNA modification, metabolite biosynthesis, and bioenergetic processes (Tsaousis, 2019).

Some enzymes involved in the TCA cycle are Fe-S cluster proteins, such as the aconitase (AcnA and AcnB), succinate dehydrogenase complex (SdhB) and fumarase (FumA and FumB) (Fontecave *et al*., 2008). Interestingly, in eukaryotes some essential proteins like aconitase (Ciccarone et al., 2019), proteins involved in the Fe-S biogenesis (IscS) (Baussier *et al*., 2020) and glyceraldehyde-3-phosphate dehydrogenase A (GapA) are the target of succination in their cysteines (Kornberg *et al*., 2018) Therefore, succination has wide-ranging effects on the metabolism on eukaryotes (Jové *et al*., 2020) but it has not been well- established for prokaryotic organisms.

For this reason, the aim of this project is to validate in *E. coli* some succination targets previously revealed by proteomics. Moreover, focus on Fe-S cluster proteins from the TCA for a better understanding of critical factors participating in cell metabolism, and the spectrum of responses that may be triggered by metabolic perturbation.

THEORICAL FRAMEWORK

The centrality of the TCA cycle for metabolism is significant as it connects all catabolic substrate oxidation pathways to the respiratory chain and it represents the source of biosynthetic products for many anabolic processes (Werner *et al*., 2016). As shown on Figure 1 (Fig 1.A.), one of the enzymes involved in the early steps of this cycle is the aconitase (Acn), which catalyzes the isomerization of citrate to isocitrate via cis-aconitate (Ciccarone *et al*., 2019). This protein is of interest for this study not only because it possesses a [4Fe-4S] iron–sulfur cluster (Castro *et al*., 2019), but also because its activity plays a crucial role in the regulation of cellular metabolism. The evidence that Acn is targeted by redox-dependent post translational modifications (PTM), both in the cytosol and mitochondria, suggests a key role for this protein in the regulation of cellular stress-induced responses (Castro *et al*., 2019).

Another important enzyme involved both in the TCA cycle and respiratory electron transfer chain is the succinate dehydrogenase (SDH) or complex II, which is a complex of four polypeptides (named A to D) encoded by the nuclear genome (Moosavi *et al*., 2019). It oxidizes succinate to fumarate (Fig 1.B), and one of its units, the SdhB, is an Fe-S cluster protein containing three Fe–S clusters ([2Fe-2S] cluster, [3Fe-4S] cluster and a[4Fe-4S] cluster) (Tondo *et al*., 2015). With the regulation of this enzyme and other complexes involved in oxidative phosphorylation, the cell is able to perform cellular respiration, hypoxic response, and other cellular activities such as gene expression (Moreno *et al*., 2020). Therefore, altered SDH activity could give rise to related consequences due to reduced electron flow, increased oxygen toxicity, and succinate accumulation (Ciccarone et al., 2019).

After SDH the subsequent enzyme is fumarase (Fig 1.C), performing the reversible hydration of fumarate to L-malate (Ciccarone *et al*., 2019). The synthesis of fumarases in *E. coli* is encoded by the genes FumA, FumB and FumC (Derbikov *et al*., 2017). Both FumA and FumB contain a [4Fe-4S] center and its exposure to oxidative agents results in damage to the metal cofactor and loss of enzyme activity (Silas *et al*., 2021).

In contrast, FumC is an iron-independent enzyme insensitive to oxidative damage and made by the cells primarily as a backup enzyme if the FumA or FumB enzymes are damaged by reactive oxygen species (ROS) (Silas *et al*., 2021; Katayama *et al*., 2019). Furthermore, it has been shown that the depletion of this enzyme leads to an increase of intracellular concentration of fumarate and succinate, as well as the interruption in the TCA cycle (Ruecker *et al*., 2017; Himpsl *et al*., 2020; Silas *et al*., 2021).
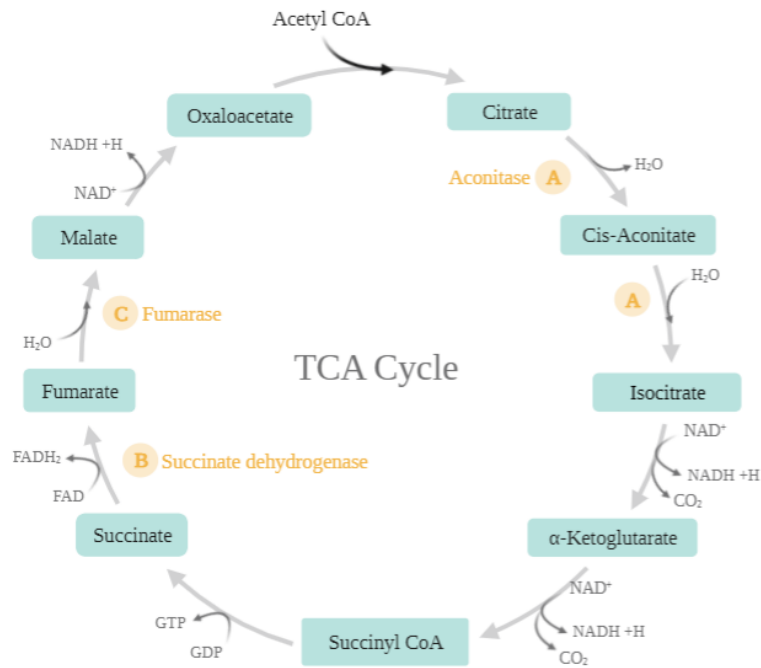
*Figure 1. Overview of the TCA cycle and the enzymes involved to be studied. A)
aconitase, B) succinate dehydrogenase, C) fumarase (Source: Own work).*

It has been proven in eukaryotic cells, specifically in Fh1 (murine fumarase)-deficient mice cells, that the loss of fumarase activity causes accumulation of intracellular fumarate, directly modifying cysteine residues to form 2SC through succination. The succination of three cysteine residues in mitochondrial Aconitase2 (ACO2) showed not only that fumarate exerts a dose-dependent inhibition of this enzyme's activity, but that the levels of succination increased as increasing fumarate concentration (Ternette *et al*., 2013). Knowing that the succinate resulting from fumarase deficiency targets and potentially alters the function of multiple proteins, it might even contribute to the

deregulation of cellular metabolism by altering other pathways or processes (Ternette *et al*., 2013).

For instance, disruption of the Respiratory Chain (RC) in human and mouse fumarase hydratase deficient cells has also been demonstrated, as fumarate induced succination of key components of the iron-sulfur cluster biogenesis family of proteins, leading to defects in the biogenesis of iron-sulfur clusters that affect complex I function. Simultaneously, fumarate accumulation decreased SDH-driven respiration by competing with succinate, having no direct inhibitory effects on complex I, but suppressing complex II activity by product inhibition (Tyrakis *et al*., 2017). All the above provides evidence that the loss of a single TCA cycle enzyme is sufficient to cause combined RC activity dysfunction.

On the other hand, in prokaryotes, succination of a few proteins (Aminopeptidase N (encoded by *pepN)*, 1,4-α-Glucan branching enzyme (encoded by *glgB)* and Catalase-peroxidase (encoded by *katG*)) has been shown for *Mycobacterium tuberculosis* when intracellular fumarate concentrations are increased (Ruecker *et al*., 2017). Moreover, proteomic preliminary results obtained at my hosting laboratory also indicate succination for *E. coli* of 8 non-containing Fe-S cluster proteins and only one Fe-S containing protein (SdhB, Succinate dehydrogenase subunit B) when fumarate is accumulated, either by deletion of the three fumarases respectively or through the exposure to metabolite analog Dimethyl Fumarate (DMF), which is thought to be modified into Monomethyl fumarate (MMF) once it enters the cell and then react with available cysteine residues (Kornberg *et al*. 2018).

One of these targets is the inosine 5'-phosphate (IMP) dehydrogenase or GuaB protein, product of the *guaB* locus in *E. coli* K12, which catalyzes the conversion of inosine 5'-phosphate to xanthosine 5'-phosphate (XMP), the first committed and rate-limiting step in the guanine nucleotide biosynthesis and therefore plays a significant role in the regulation of cell growth and proliferation (Fotie, 2018). Another target of succination and related to GuaB corresponds to the guanosine monophosphate (GMP) reductase,

encoded by *guaC*, it catalyzes the conversion reaction of GMP to IMP which is part of the purine salvage pathway and is important in the conversion of nucleoside and nucleotide derivatives of guanine to adenine nucleotides (Imamura *et al*., 2020).

Also, GlnA or glutamine synthetase (GS) which produces glutamine from glutamate and ammonia and has a crucial part in nitrogen metabolism (Millanao *et al*., 2020) was identified as a target of succination.

Finally, GapA (glycerol 3-phosphate dehydrogenase A), which encodes an essential component of the glycolytic pathway which catalyzes the conversion of glyceraldehyde 3-phosphate to glycerate-1,3-bisphosphate, and results in production of NADH (Wang et al., 2020) was observed in our preliminary succination study and is a known target of succination in eukaryotes (Kornberg *et al*., 2018).

The fact that the proteins mentioned above have been detected as succinated in unpublished data and play a fundamental effect on cell growth and viability makes them measurement subjects for the validation of succination by fumarate in prokaryotes, to corroborate its effects and how these alterations may impact cells growth and functions.

OBJECTIVES

GENERAL OBJETIVE

Validate succination targets discovered by proteomics and its effects on *Escherichia coli* as model organism.

SPECIFIC OBJECTIVES

1.   Test genetically modified *E. coli* strains by exposure to fumarate analogs DMF and MMF by measuring absorbance and cell growth.

2.   Establish chemical rescue tests for these strains with the addition of supplements to measure their survival.

3.   Measure the activity of succinate target proteins containing Fe-S clusters by enzymatic assays *in vivo*.

METHODOLOGY

All the procedures and tests were performed during the period of September 1st, 2021 to January 15th, 2022, in the installations of the Stress Adaptation and Metabolism in Enterobacteria (SAMe) Unit of Institut Pasteur, Paris, France.

General microbiological procedures

E. coli K-12 strain MG1655 derivatives were used along the project, selected from the strain collection of the Stress Adaptation and Metabolism in Enterobacteria Unit of Institut Pasteur, Paris, France. Strains were codified as follows: a. Wild-type (WT), b. Δ*fumABC,* c. Δ*iscUA* and d. Δ*sufBCD* (Table 1).

Table 1. Code and genotype of the *E. coli* K-12 strain MG1655 derivatives used for the tests.

Strain	Genotype
WT	MG1655 Parental strain
Δ*fumABC*	MG1655 Δ*fumABC*
Δ*iscUA*	MG1655 Δ*iscUA::catDV597*
Δ*sufBCD*	MG1655 *DsufBCD::kan*

The media used for the bacterial cultures were LB Miller (liquid and agar plates) and M9 minimal medium supplemented with glycerol (0.2%). The LB Miller medium composition was 10 g/L of tryptone, 10 g/L of NaCl and 5 g/L of yeast extract (Sigma-Aldrich, n.d.). The M9 medium (500 mL) was prepared with 50 mL of M9 solution 10X (11.32g Na_2HPO_4, 3g KH_2PO_4, 1g NaCl, 2g NH_4Cl and ddH_2O to 100 mL (Shakeel *et al*., 2020)), 1 mL of $MgSO_4$ 1M, 1.25 mL of $CaCl_2$ 40 mM, 0.1 mL of Thiamine 10 mg/mL, 2 mL of Glycerol 50% and 440.7 mL of H_2O (protocols obtained from laboratory).

To determine the effect of succination on bacterial physiology, two approaches were followed: A) Validation of succination targets (containing or not Fe-S clusters) by

chemical recue tests on mutants and measuring absorbance and growth behavior, and B) Validation by testing two systems for fumarate accumulation in combination with enzymatic assays specifically for the Fe-S containing proteins.

A. VALIDATION BY CHEMICAL SUPPLEMENTATION IN MUTANTS

1. Construction of genetic tools

For the *E. coli* strains not available in the laboratory collection, a transduction protocol and a Datsenko & Wanner method were followed for their transformation.

1.1. Datsenko-Wanner protocol for ΔgapA:

The "One-step inactivation of chromosomal genes in *Escherichia coli* K-12 using PCR products protocol (Datsenko & Wanner, 2000) was followed, using pKD13 as DNA template and the following primers:

Table 2. Construct primers for internal overlap with sequence homologous to the ends in the target.

Primer	Sequence	Length
gapA forward	ATTTTACAGGCAACCTTTTATTCACTAACA AATAGCTGGTGGAATATATGATTCCGGGG ATCCGTCGACC	70 bases
gapA reverse	CTCTTTTTAGATCACAGTGTCATCTCAACT TATTTGGAGATGTGAGCGATTGTAGGCTG GAGCTGCTTCG	70 bases

1.2. Transduction with P1 bacteriophage for ΔguaB, ΔguaC, ΔglnA

The strains used for the P1 transduction were obtained from the Keio collection, a knockout collection with a set of precisely defined, single-gene knockouts by a kanamycin resistance cassette using the Datsenko & Wanner method (Baba *et al*.,

2006). The deleted genes (*guaB*, *guaC* and *glnA*) in this collection contain a kanamycin insert, which was used for the selection process.
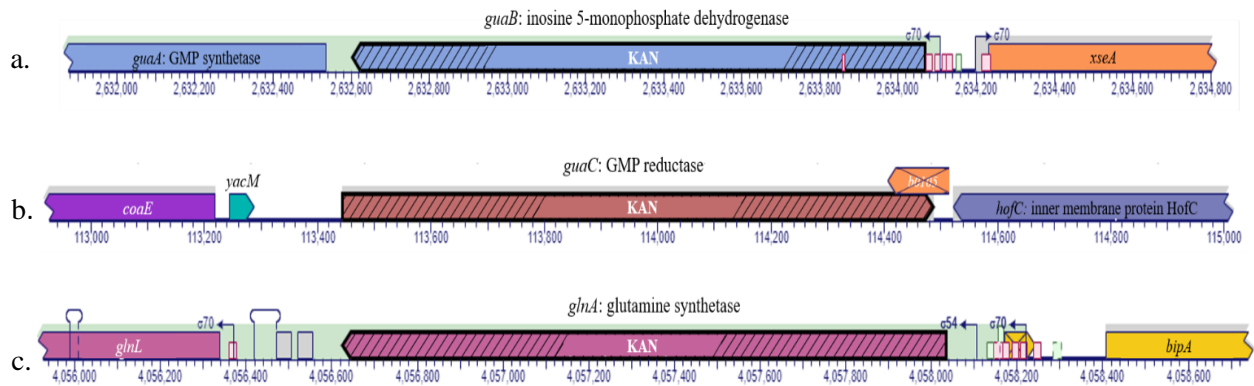
Figure 2. Kanamycin (KAN) cassette inserted in the respective locus by transduction with P1 phage of: a) guaB, b) guaC and c) glnA (Source: BioCyc).

The protocol described by Thomason *et. al.* (2007) was followed. For the preparation of the P1 lysate, each strain donor (*E. coli* K-12 wild-type BW25113 background) was cultured overnight (ON) in 3 mL of 2XYT (Yeast Extract Tryptone) medium and 3 µL of 50 µg/mL kanamycin. A 1/100 dilution from the ON culture was prepared in 3 mL of 2XWT and 150 µL of CaCl$_2$ 0.1M and incubated at 37°C with agitation. Once reached an optical density at 600nm (OD$_{600}$) between 0.5-1, 150uL of P1 WT lysate were added, and incubated again at 37°C without agitation for 20 minutes, and then switched to agitation for 3-4 hours. Next, 300 µL of chloroform were added and incubated at 37°C with agitation for 15 minutes, then centrifuged 10 minutes at 4°C at 6000rpm. Finally, 15 µL of chloroform were added.

For the transduction, the receptive strain (*E. coli* K-12 wild-type MG5565) was cultured ON in 3 mL of 2XWT. A 1/50 dilution from the ON culture was prepared in 3 mL of 2XWT and 150µL of CaCl$_2$ 0.1M and incubated at 37°C with agitation until reaching an OD$_{600}$ of 1. Next, 500 µL of these cells were distributed in three Eppendorf tubes and added 0 µL, 10 µL and 100 µL of the P1 lysate. After infecting during 20 minutes at 37°C without agitation, 1 mL of sterile LB-citrate 5 mM was added, and incubated again during 50 more minutes with agitation at 700-750 rpm. Then,

centrifuged 5 minutes at 5000 rpm at room temperature, removed the supernatant and resuspend in 1 mL of sterile LB-citrate 5mM. The centrifugation was repeated and resuspended the obtained pellet in 100 µL LB-citrate 5mM. Finally, the cells were spreaded on LB Agar-AB plates (with 50 µg/ mL kanamycin and 2 mM citrate). Colonies were reisolated twice.

For the verification of the transduction a PCR was made using the Q5 High-Fidelity 2xMaster Mix and protocol by New England BioLabs, with the following components: DNA template corresponding to the knockout clones obtained, 25 µL of the Q5 High-Fidelity 2xMaster Mix (containing Q5 DNA Polymerase and) 1.25 µL of 10 µM Forward and Reverse primers and nuclease-free water up to 25 µL per reaction. The primers for verification were designed and provided by the hosting lab. The respective sequences are shown below:

Table 3. Designed primers for PCR transduction verification and PCR product's size.

Primer	Sequence	PCR size (bp)
guaB forward	CCTGTCCCATCTCATGCTCAAG	1923
guaB reverse	GAATTTGTGCTTCTGTCACATCCC	
guaC forward	CAATGCCTCCCGTTAAGGCAAC	1492
guaC reverse	CATCATCGGGAAAACACAATGGCG	
glnA forward	CAGATTTCGTTACCACGACGACC	1563
glnA reverse	GTAGGCCGGATAAGACGCATTTG	

A flanking reverse primer was also for the verification of the clones, in which when performing the PCR will only amplify if the kanamycin cassette was inserted with an estimated product of ~750bp (Figure 3).
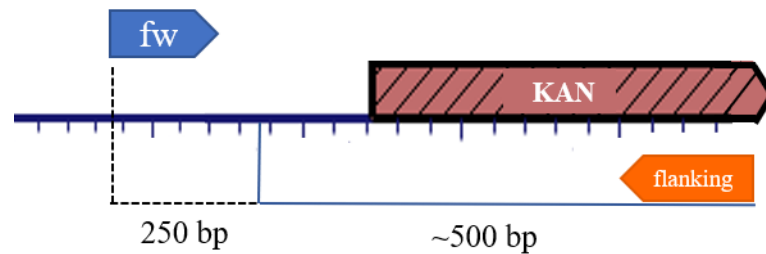
Figure 3. Representation of primers binding at flanking region of the locus, where fw corresponds to each clone's respective forward primer and flanking to a reverse primer complementary to a region of the resistance cassette sequence.

To check both 1.1 and 1.2. recombinations, a verification by PCR was performed for each, either by product´s size difference or using a flanking primer.

2. Chemical rescue tests in mutants

Once obtained the Δ*guaB,* Δ*guaC* and Δ*glnA E.coli* mutants, each strain was cultured ON in 3 mL of LB medium at 37°C and 200 rpm. The OD_{600} was measured and spined down 1 OD unit (3 minutes at 3000rpm). The obtained pellet was washed twice with M9 glycerol 0.2% and finally resuspended again to 1 OD unit in this medium.

96 well plates were used to set the bacterial cultures. Each culture was prepared by inoculating a final value of 0.1 OD_{600} from the previous liquid culture left ON on 200 µL of M9 glycerol 0.2% media with the different supplement's concentrations.

Supplements were added to each according to their respective deficiencies: Δ*guaB* was supplemented with xanthine in concentrations of 20 µg/mL, 10 µg/mL, 5 µg/mL, 2.5 µg/mL, 1.25 µg/mL, 0.62 µg/ml and 0 µg/ml; Δ*guaC* was supplemented with adenine in concentrations of 100 µg/ml, 50 µg/mL, 25 µg/mL, 12.5 µg/mL, 6.2 µg/mL and 0 µg/mL; Δg*lnA* was supplemented with glutamine in concentrations of 10 mM, 5 mM, 2.5 mM, 1.25 mM, 0.62 mM, 0.31 mM, 0.15 mM and 0 mM.

Consequently, measures of the absorbance (OD_{600}) and growth curves were made after 16 hours incubating at 37°C and 200 rpm in a Microplate Reader.

3. Exposure to DMF/MMF and determination of MIC

The minimal inhibitory concentration (MIC) for the DMF and MMF was determined with growth tests and absorbance measurement of the mutants in a Microplate Reader, by adding different concentrations of these analogues to M9glycerol 0.2% and LB medium. The concentrations of DMF tested were 5 mM, 2.5 mM, 1.25 mM, 0.62 mM, 0.31 mM and 0 mM, and for MMF were 30 mM, 15 mM, 7.5 mM, 3.75 mM, 1.87 mM and 0 mM. DMSO (Dimethyl Sulfoxide) was used as a control since both solutions of DMF and MMF were solubilized with DMSO. Once the optimal concentration of each supplement was known, tests were repeated by exposing each strain to both DMF/MMF together with the respective supplement. Final optical density at 600nm was measured after 16 hours using a Microplate reader in a 96 well plate.

4. Chemical rescue tests in WT and Δ*fumABC E. coli* strains plus exposure to DMF/MMF

Using the established supplements concentrations, WT and Δ*fumABC* strains were tested on LB, M9 glycerol 0.2%, M9 glycerol 0.2% with each supplement individually added and M9 glycerol 0.2% with all supplements added together (GAX), plus exposure to DMF/MMF. Growth curves were evaluated after 16 hours using the MICROPLATE READER.

B. VALIDATION BY ENZYMOLOGY IN FE-S CLUSTER PROTEINS

1. Pretreatment of cells

WT and Δ*fumABC E. coli* strains were evaluated in this test. For the pretreatment of the cells, each strain was grown ON in 3 mL of LB growing at 37 and 200rpm, then refreshed (1/50 dilution) in two separate Erlenmeyer tubes with 25 mL of LB and grown at the same conditions. Once reaching an OD_{600} of 0.6-0.7, DMF at 2.5 mM was added to one culture and DMSO as a control to the other one. Both cultures were grown two more hours.

To start from the same cell density, the OD_{600} for both treatments was measured and spined down 1.5 OD units during 10 minutes at 4000 RCF. While keeping on ice, the pellet was resuspended in 1 mL of Tris-HCl and sucrose 0.5M. Cells were lysed by adding 0.1 mL of lysozyme (at a concentration of 2mg/mL in EDTA 0,1M) and 0.9 mL of these cells. After left 20 minutes on ice, cells were centrifuged 5 minutes at 1000rpm, and pellet was held frozen at -20°C.

2. Enzymology tests

To measure the enzymatic activity of fumarase and aconitase, a direct assay by absorbance measurement was performed.

To finish the lysis of the cells pretreated with DMF and DMSO, these were thawed for two minutes at room temperature, resuspended in 1 mL of cold water and finally sonicated. Immediately after completing the lysis, a cuvette was loaded with 50 μL of lysed cells and 3 mL of buffer according to the enzyme to be tested. Absorbance was measured at 240nm. For the fumarase, the substrate buffer was prepared with 15 mL Tris-HCl 50 mM, 8 mL $MnCl_2$ 1M and 0.3 mL isocitrate 0.5M (final concentration of 20 mM). For the aconitase, the substrate buffer was prepared with KH_2PO_4 100 mM, pH 7.6 and malate 50 mM.

Using a UV-Visible spectrophotometer, enzyme's kinetics was followed by measuring absorbance at 240nm on intervals of 1 second during 120 seconds, taking the slope of the linear part of the curve describing the rate of change in the formation of product monitored. The measure of absorbance (corresponding to the double bond on the cis-aconitate intermediate and reverse reaction by malate) was performed as a direct assay to calculate the concentration of these metabolites. Enzyme activity was then calculated from the change in absorbance per unit of time.

3. Protein quantification

Protein concentration was determined by Bradford Assay following the Bio-Rad Protein Assay catalog protocol (Bio-Rad Laboratories, Inc. 2005). For the specific

activity, the final concentration of aconitate and fumarate was obtained by Beer-Lambert's law following the next equation:

$$A = \varepsilon \, l \, c \quad [1]$$

Where A is the absorbance obtained, ε at 240nm corresponds to 3,6 mM^{-1} cm^{-1} for aconitate and 2,44 mM^{-1} cm^{-1} for fumarate, l is the cuvette's length and c the concentration to find.

C. DATA ANALYSIS

Finally, the data obtained was analyzed using Excel and graphs were created using the software GraphPad Prism 9.3.1.

RESULTS AND DISCUSSION

Verification of constructs

As a first step prior to performing the supplementation tests, we needed to construct strains deficient in the studied genes, which would be used as reference for the effect of DMF in that specific target or pathway and could be possibly restored by exogenous chemical incorporation. Then, we proceed to transduce those deletions into our laboratory strain MG1655 (from KEIO BW25113) as shown in Figure 2, and verified the correct transduction of those knockouts by PCR, comparing the difference in sizes between products (Figure 4). A DNA ladder was used as reference for the electrophoretic run.

First, when analyzing the Δ*guaB*, all three clones showed amplification and bands slightly less than 2kb. Therefore, the correct insertion by size difference is verified as the WT presented a bigger size band around 2kb, similar to the size of the expected PCR product (1923bp as indicated in Table 3). Likewise, Δ*guaC* was verified correctly by amplifying slightly less than 2kb, and comparing band's size difference, WT band was about 1.5kb, which matches with the expected PCR product of 1492bp. However, for the Δ*glnA* clones, the bands showed a size of 1.5kb, equal to the expected product size for WT (1563bp). Therefore, there was no size difference and the correct insertion of the resistance cassette cannot be determined.
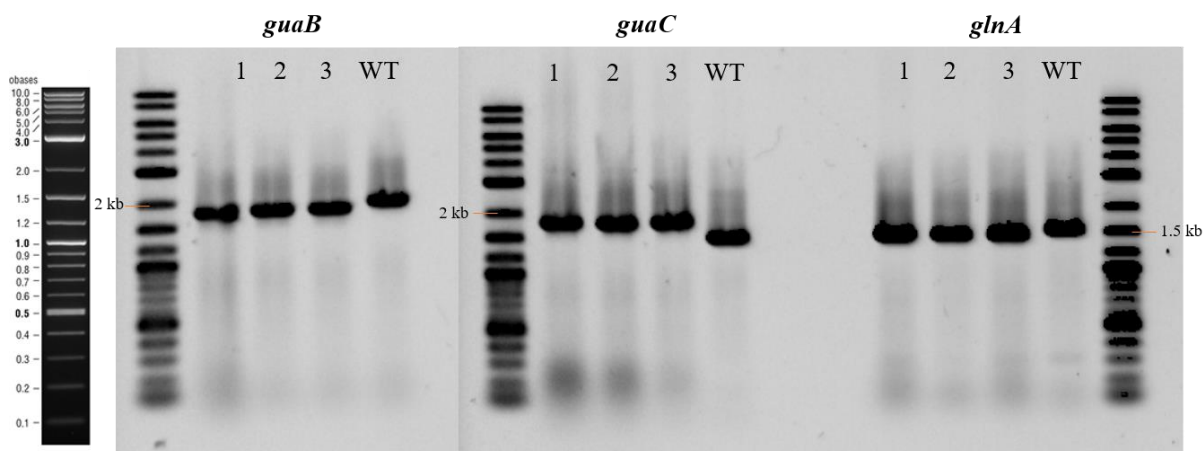
Figure 4. Electrophoretic run for PCR verification of phage transduction in ΔguaB, ΔguaC and ΔglnA clones, where lanes 1, 2 and 3 correspond to samples of each strain and lane 4 to WT control.

Given the above, a PCR was repeated using a flanking primer within the kanamycin cassette. This electrophoresis (Figure 5) showed bands around slightly less than 1.2kb for ΔguaB and ΔguaC clones and 1kb for ΔglnA, corresponding to the region amplified by the primers (~750bp as shown in Figure 3). There should have been no amplification in for the WT samples, as by using the flanking primer it will amplify if the cassette is inside the targeted region. However, the WT sample for the ΔglnA electrophoretic run presented a very faint band, which can be assumed the primer is non-specific.
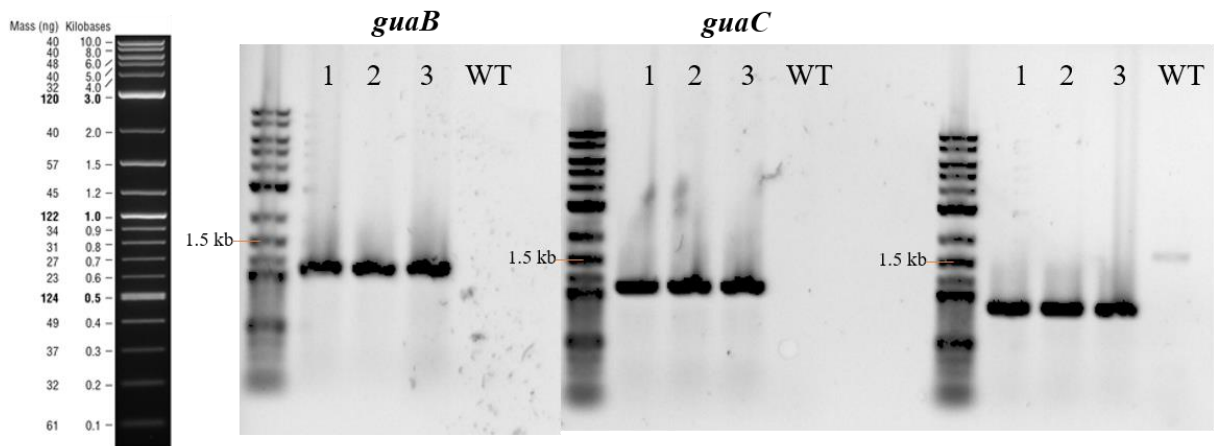
Figure 5. Electrophoretic run for PCR verification of phage transduction in ΔguaB, ΔguaC and ΔglnA clones using flanking primer, where lanes 1, 2 and 3 correspond to samples of each strain and lane 4 to WT control.

On the other hand, Datsenko-Wanner protocol was followed with the aim of obtaining a Δ*gapA* mutant. As mentioned before, GapA (glycerol 3-phosphate dehydrogenase) is a known target of succination in eukaryotes (Korberng *et al*., 2018). Despite it being essential under normal growth conditions, it has been proven it could be bypassed by growing with glycerol plus Succinate or Casamino Acids as carbon source (Seta *et al*., 1997). Even by following previously reported growth conditions, we were unable to obtain these mutants, which can be due to the accumulation of toxic intermediates (Baba *et al*., 2006). The above also evidenced the vitality of this gene for the survival of the bacteria.

Chemical rescue tests: Supplementation

Knowing that GuaB, GuaC GlnA proteins are succination targets, the first test to validate this was the exposure of these mutants to DMF, as it is analogous to fumarate. It was also considered whether their respective chemical complementation could be achieved once DMF or fumarate is added. To accomplish this, each mutant was supplemented according to its respective auxotrophy in order to determine the quantity needed to be added for the regeneration of the activity.

Regarding $\Delta guaB$ this is a xanthine auxotroph (Keller & Simon, 1987), so xanthine supplementation has been reported to enable growth when added to defined medium at final concentration of 20ug/mL (Lambden & Drabble, 1973). Following the above, these mutants were grown in minimal medium and xanthine was added at concentrations from 20 µg/mL to 0.62 µg/mL as indicated in Figure 6. The final absorbance measurement after 16 hours of incubation showed that the highest average OD_{600} value (0.298) was reached when supplemented at a concentration of 5 µg/mL (Fig. 6.a.). Similarly, supplementation is evident when looking at the growth curve (Fig. 6.b.), where a greater exponential growth is seen at this concentration, compared to the medium with the other concentrations and without adding xanthine. By considering WT as a control because it grows in minimal medium (Sezonov *et al*., 2007), it does not show any difference between final OD values if supplemented or not.
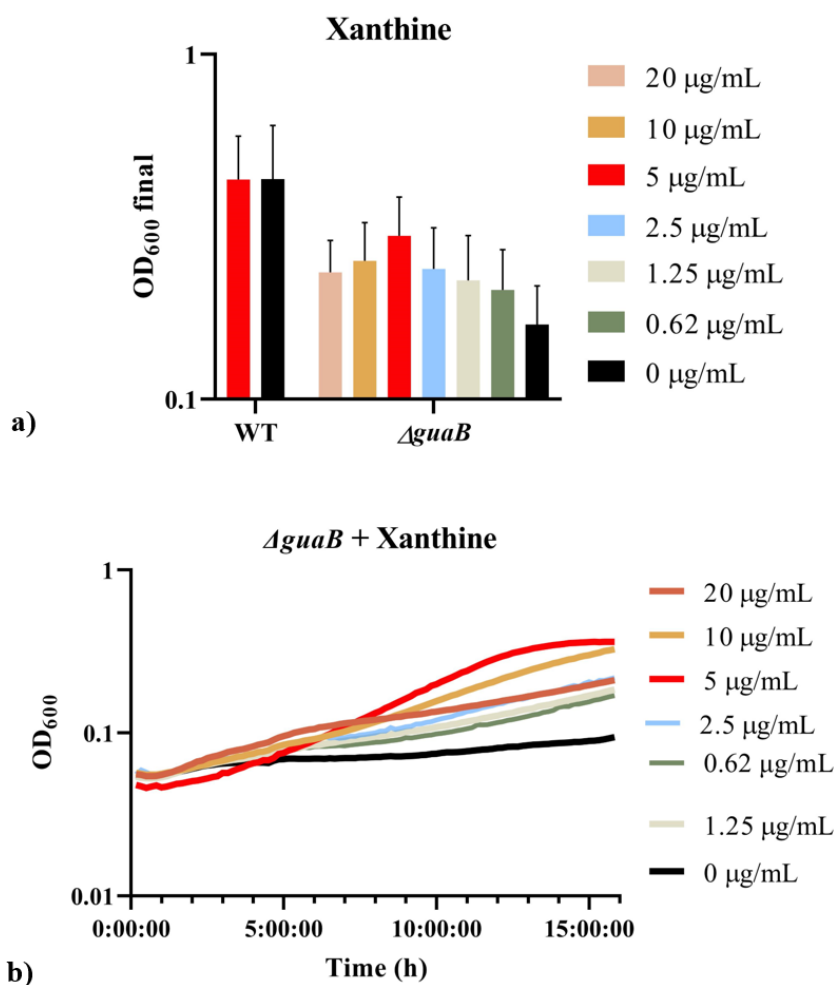
Figure 6. E. coli ΔguaB mutant grown in M9 minimal medium with the indicated concentrations of xanthine added. Final measurements after 16 hours in a Microplate Reader corresponding to: a) Absorbance reached (OD_{600}) compared to WT strain, b) Growth curve plot.

It has also been demonstrated the growth of Δ*guaC* mutants upon addition of adenine or hypoxanthine (Kessler & Gots, 1985). Adenine was added to the minimal medium at concentrations of 100 µg/mL to 6.2 µg/mL, as indicated *in* Figure 7. From the final absorbance measurement (Fig. 7.a.), the concentration of 50 µg/mL indicated the highest average value (final OD of 0.256), being slightly higher than the value given when no supplement is added to the medium (OD of 0.226 for 0 µg/mL of adenine).

This complements the growth tendency (Fig. 7.b.), in which this concentration shows the highest exponential growth, while no change is shown when no supplement is added, indicating a sudden arrest of cell growth. Nevertheless, the mutant could not grow to wild-type levels even when supplemented.
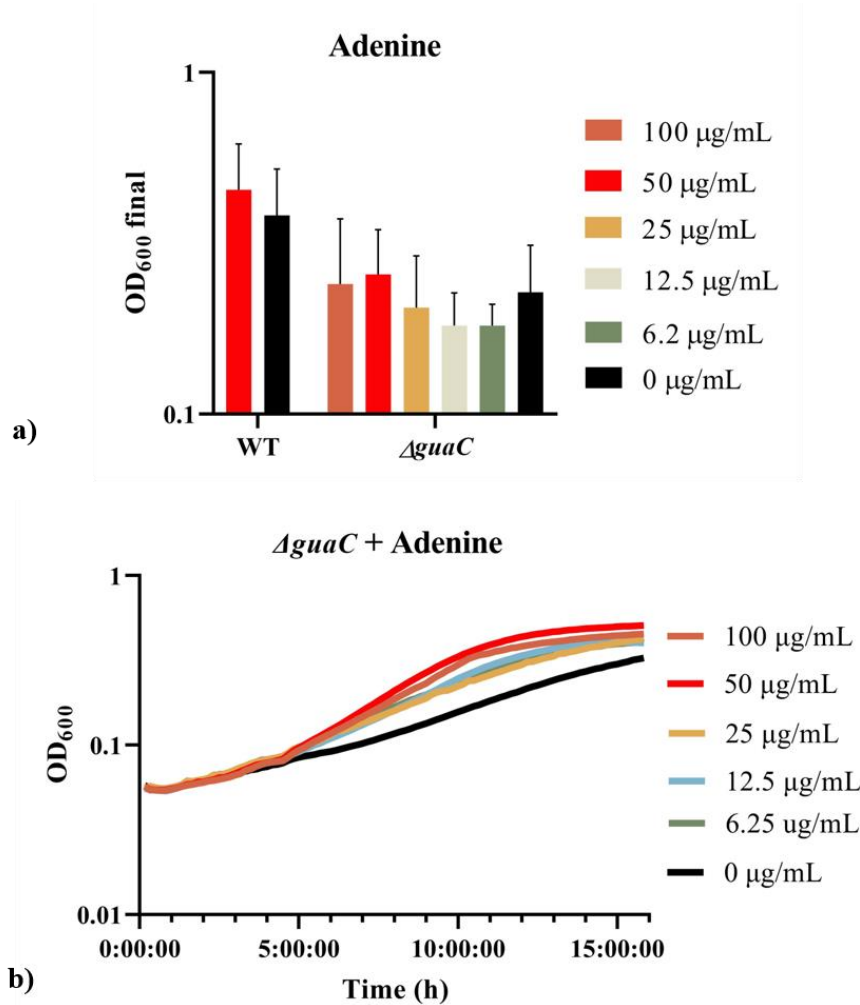
Figure 7. E. coli ΔguaC mutant grown in M9 minimal medium with the indicated concentrations of adenine added. Final measurements after 16 hours in a Microplate Reader corresponding to: a) Absorbance reached (OD_{600}) compared to WT strain, b) Growth curve plot.

On the other hand, the inactivation of GlnA results in an absolute glutamine requirement (Margelis *et.al.*, 2001). This mutant was grown in minimal medium supplemented with this amino acid at concentrations between 5 mM and 0.15 mM (Figure 8) as literature reports these glutamine levels are required to supplement the glutamine auxotrophy (Margelis *et.al.*, 2001). According to the final absorbance, 5 mM is the concentration whose supplementation is higher, indicating a higher OD (Fig. 8.a.). For the WT, glutamine appears not to supplement it, as the final OD reached is similar when it is supplemented or not. The growth curves shows that the lower the glutamine concentration, the lower the final OD reached (Fig 8.b.).
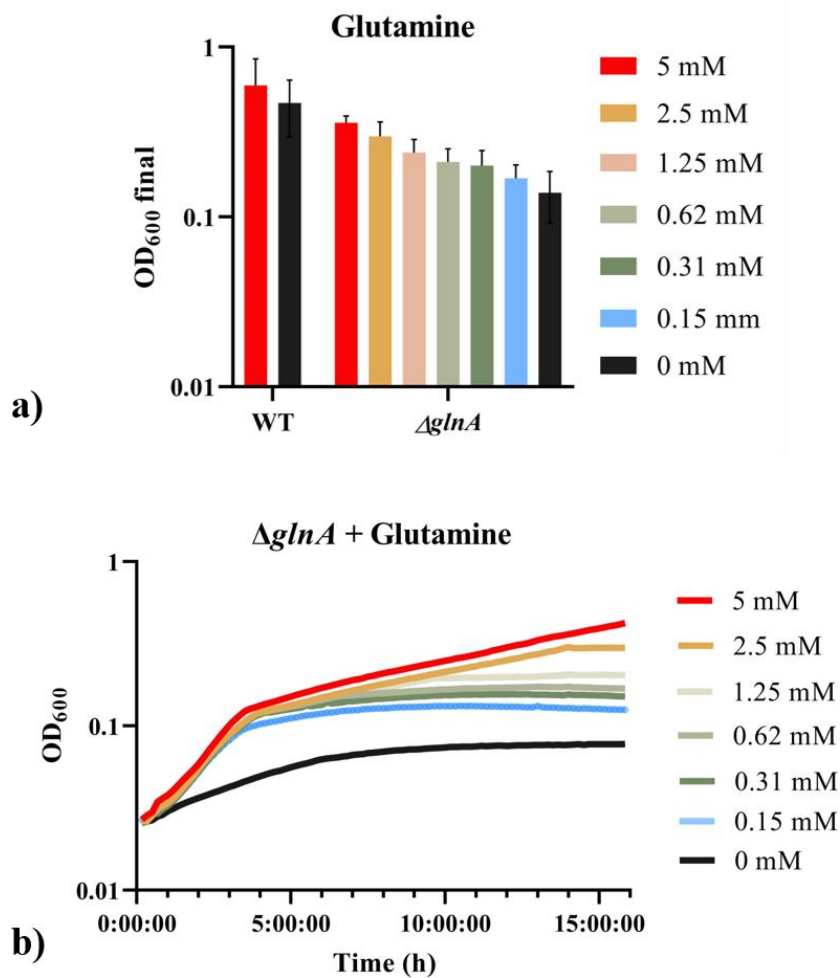
Figure 8. E. coli ΔglnA mutant grown in M9 minimal medium with the indicated concentrations of xanthine added. Final measurements after 16 hours in a Microplate Reader corresponding to: a) Absorbance reached (OD600) compared to WT strain, b) Growth curve plot.

It was determined to this point that concentrations of 5 µg/mL of xanthine for Δ*guaB*, 50 µg/mL of adenine for Δ*guaC* and 5 mM of glutamine for Δ*glnA* achieved supplementation of the mutants.

Exposure to fumarate analogs

a. Mutants

Once the concentration that best supplemented each mutant was known, DMF exposure was proceeded. Being a fumarate ester, DMF is widely used as a drug for the treatment of human diseases (Linker & Haghikia 2016; Kourakis *et al.*, 2020). Although its mechanisms of action remain incompletely understood, it is known to covalently modify cysteine residues by succination (Blewett *et al.*, 2016), and data has reported not only fumarate accumulation but a killing effect (Ruecker *et al.*, 2017). For the tests, concentrations of 5 mM, 2.5 mM, 1.25 mM, 0.62 mM, 0.31 mM and 0 mM of DMF were used. When growing the three strains on LB medium, 2.5 mM was determined as the minimal inhibitory concentration (MIC) for the DMF. This medium was used for the experiments as it is a nutrient-rich, partially defined medium that is widely used for *E. coli* cultures as the WT strain grows rapidly (generation time is 20 minutes) (Sezonov *et al.*, 2007; Suzuki *et al.*, 2019).

In the same way the three mutants showed growth in LB medium (Gerdes *et al.*, 2003). As for the Δ*glnA* and Δ*guaB*, it has been reported they do not grow in M9 medium (Joyce *et al.*, 2006). M9 medium is a defined, minimal medium also for *E. coli*, and one of the simplest media in common use, providing a bare-bones complement of phosphorous, nitrogen, and sulfur (Elbing & Brent, 2019). However, when glycerol 0.2% as carbon source and each supplement were added to M9, the mutants showed growth and different MIC values than those established in LB. The MIC values are indicated in Figure 9.
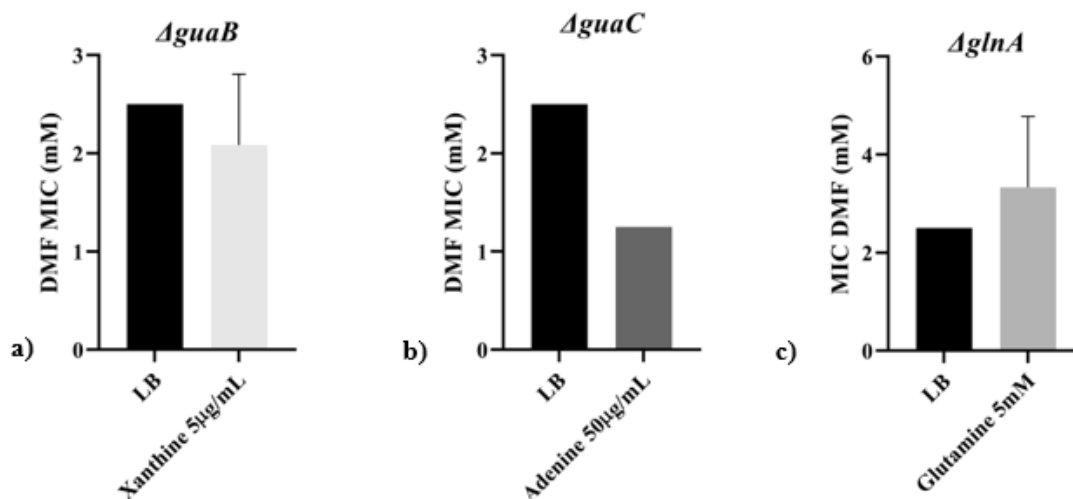
Figure 9. MIC values (mM) obtained upon exposure to DMF in LB medium and supplemented minimal medium in mutants a) ∆guaB, b) ∆guaC and c) ∆ glnA.

b. WT

When WT was exposed to DMF, MIC also corresponded to 2.5 mM when grown in LB medium. It was also observed that the MIC increases when all three supplements are added together to the minimal medium, as opposed to when they are not (Fig. 10.a.). However, the final OD measurement did not provide sufficient information to know if there is really compensation and if such supplements could bypass the effect of DMF.

In the case of the monomethyl fumarate (MMF), this has been reported as DMF's active form (Gillard *et al*, 2015), so it could be hypothesized that its exposure could also cause a toxic effect on bacteria. Also, it has been proven that treatment of the recombinant human GAPDH with MMF led to monomethyl succination (2-monomethyl succinyl-cysteine) (Kornberg *et al*., 2018), which is why it was also used for these tests. The concentrations tested were 30 mM, 15 mM, 7.5 mM, 3.75 mM, 1.87 mM and 0 mM. According to the final absorbance, the MIC for WT when exposed to MMF was 15 mM both for growth alone in M9glycerol medium and if the three supplements were added simultaneously (Fig. 10.b).
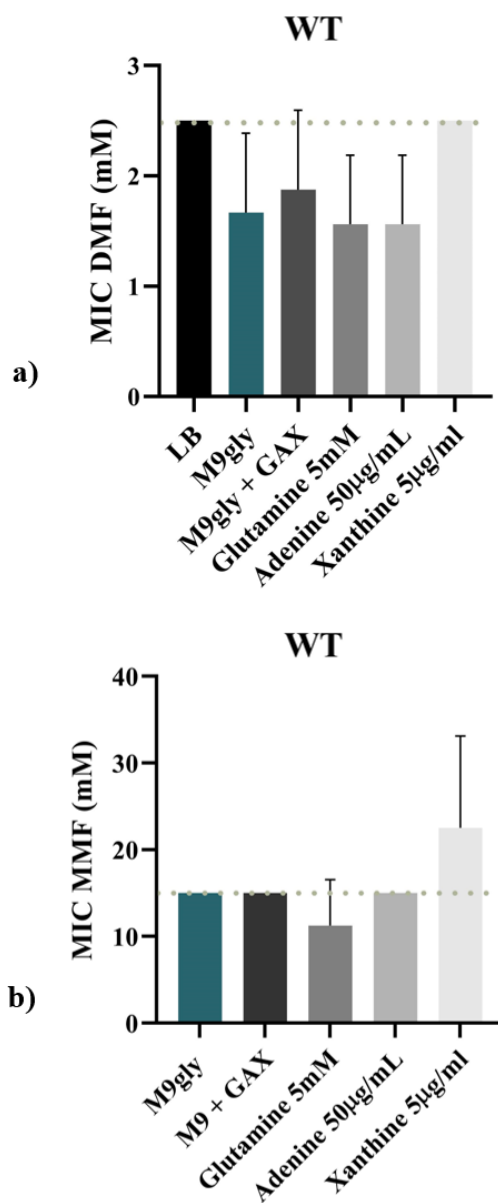
Figure 10. MIC values (mM) obtained upon exposure of WT to a) DMF and b) MMF. Mediums tested were LB, M9 glycerol 0.2% and M9 glycerol 0.2% with supplements individually and added all together (GAX).

When observing the growth behavior of WT upon exposure to DMF, the killing effect is evident upon exposure to the highest concentrations, resulting in toxicity. Whether supplementing or not (Fig. 11.a. and 11.b.), at concentrations of 5 mM and 2.5 mM no

growth is observed, confirming its role as a bacteriostatic agent (Bernatová *et al*., 2013). However, an improvement in growth is observed when exposed to DMF and all three supplements are added, but not at the previously determined MIC but going to the sub-MIC concentrations which were 0.31 mM, 0.62 mM and 1.25 mM (Figure 11.c).
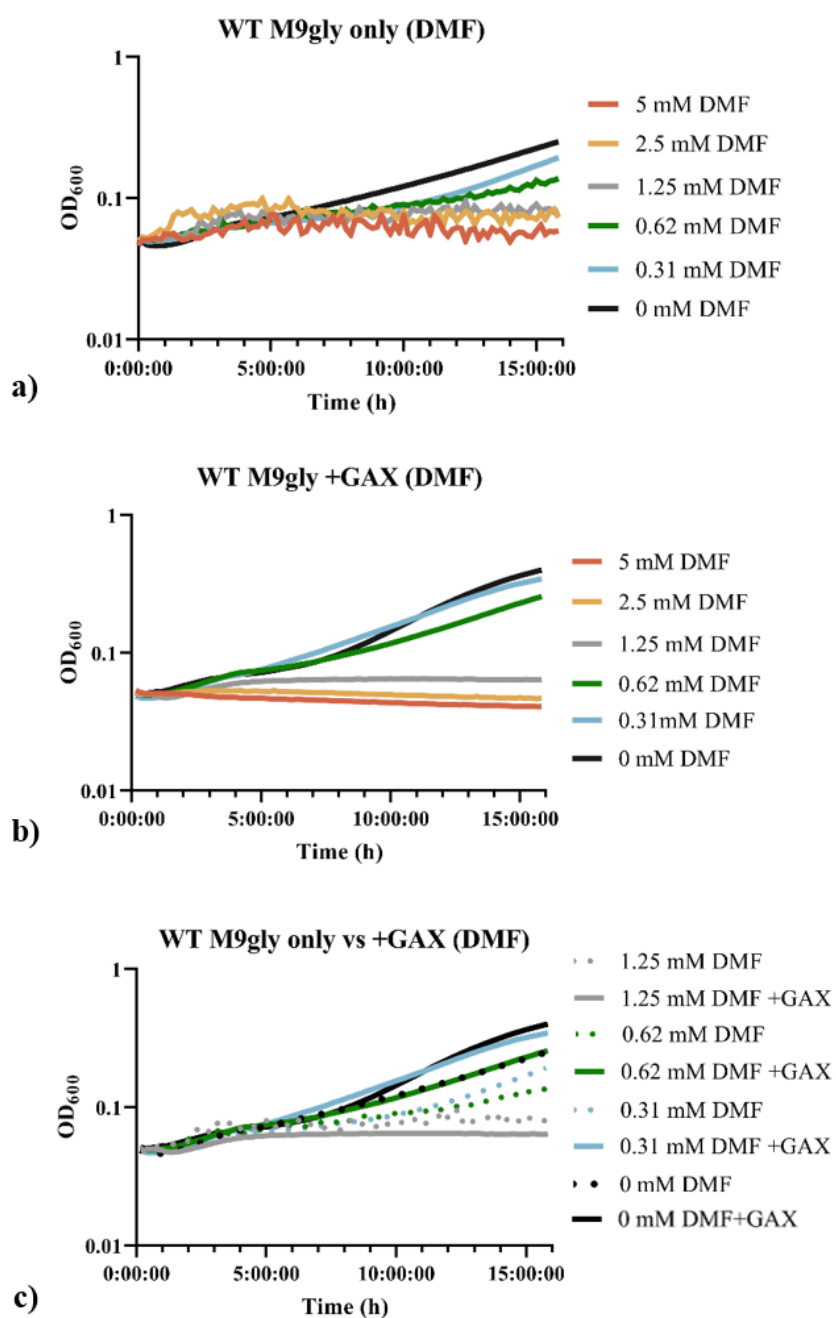
Figure 11. WT growth curves when exposed to DMF in a Microplate Reader for 16 hours: a) Growth in M9glycerol without supplementation, b) Growth in M9glycerol with the three supplements (GAX) and c) Growth in M9glycerol with the three supplements (GAX) at sub-MIC concentrations.

Comparatively, when exposing WT to MMF the behavior is the same, the higher the concentration, the lower the growth (Fig. 12.a. and 12.b.). Nevertheless, when looking at sub-MIC levels there is no improvement in growth, and a similar final OD is reached whether supplemented or not. In previous studies conducted in the host laboratory (by viable cell count over time of the WT strain), it was determined that MMF caused bacterial death, so it can be classified as a bactericidal agent (Bernatová *et al*., 2013). However, a higher effect of MMF was expected, and these results may be due to the fact that the drug is not causing succination as hypothesized, which allows WT growth in minimal medium, whether supplemented or not.

That a higher concentration of MMF than DMF is required to inhibit growth is consistent with what Kornberg *et al*., (2018) showed, as MMF promoted monomethyl succination of the active site cysteine (Cys-152) and two other cysteines (cysteines 156 and 247) in recombinant human GAPDH, whereas DMF induced a combination of dimethyl and monomethyl succination at the same three cysteine residues.
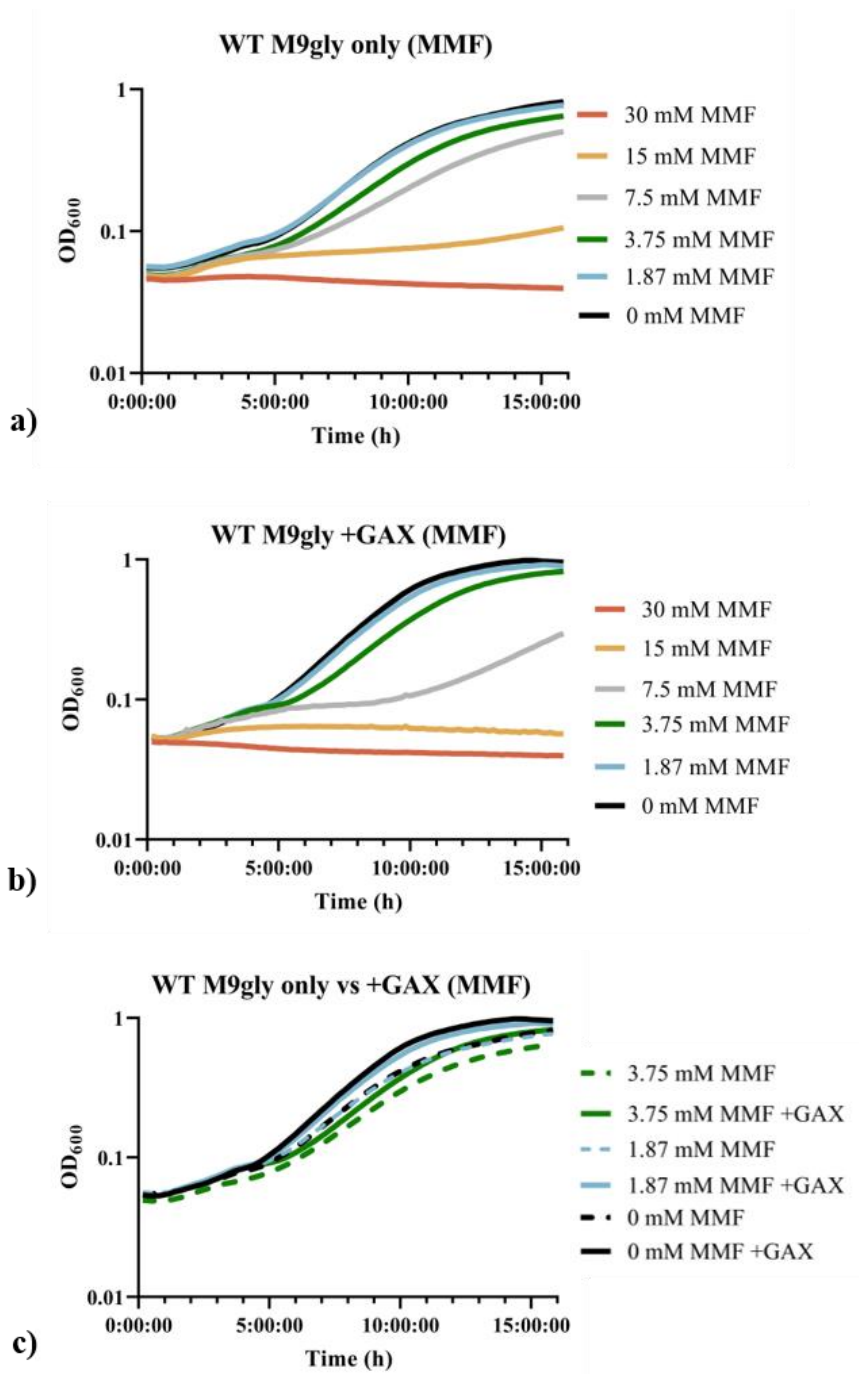
Figure 12. WT growth curves when exposed to MMF in a Microplate Reader for 16 hours, a) Growth in M9glycerol without supplementation, b) Growth in M9glycerol with the three supplements (GAX) and c) Growth in M9glycerol with the three supplements (GAX) at sub-MIC concentrations.

c. ΔfumABC

Finally, the growth behavior of the Δ*fumABC* was evaluated as it has been shown in other bacteria such as *Mycobacterium tuberculosis* that by depletion of Fum, there was succination by accumulation of fumarate (Ruecker *et al*., 2017). On the other hand, the loss of fumarase has also been associated with the increased production of reactive oxygen species (ROS), and the accumulation of fumarate in Fum-deficient eukaryotic cancer cell lines leads to the formation of an adduct between fumarate and glutathione (GSH), which depletes intracellular NADPH and enhances oxidative stress (Zheng *et al*., 2015).

As a reference of the previous tests, it was supplemented with glutamine, adenine, xanthine individually and an improvement in growth was observed compared with each compared to the growth only in M9glycerol (Figure 13).
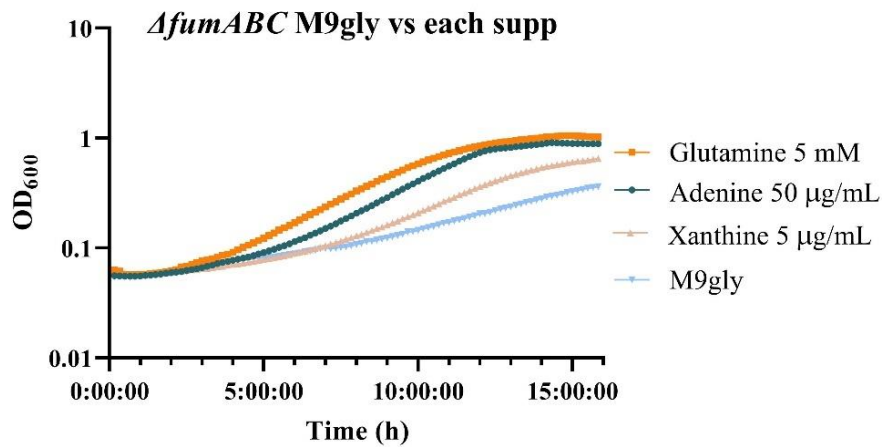
Figure 13. ΔfumABC growth curves when cultured in M9glycerol with glutamine 5 mM, adenine 50 µg/mL, xanthine 5 µg/mL and no supplement in a Microplate Reader for 16 hours.

Given that this first methodological part was based on the validation by growth, it was possible to prove that with GAX supplementation, the Δ*fumABC* mutant achieves the WT level growth, bypassing the stressor effect exerted by fumarate (Figure 14).

Δ*fumABC* and WT M9gly only vs +GAX

Legend:
- ·· Δ*fumABC* M9gly
- —— Δ*fumABC* M9gly +GAX
- ·· WT M9gly
- —— WT M9gly +GAX
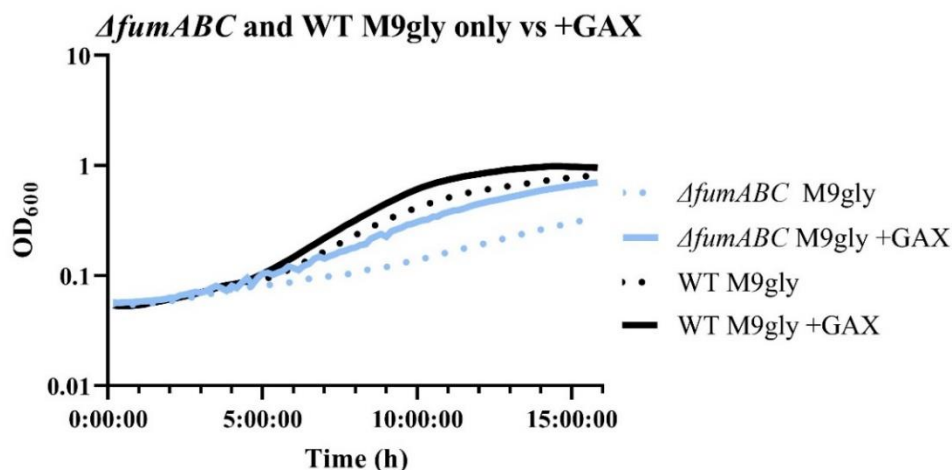
Figure 14. Comparison between WT and ΔfumABC growth curves when cultured in M9glycerol vs M9glycerol supplemented with GAX in Microplate Reader for 16 hours.

All things considered, it was shown that the same chemical rescue in growth is not achieved if exposed to DMF, MMF or if the Δ*fumABC* mutant is tested. For instance, the effect of DMF seems to be higher than if the fumarases are eliminated, as no further supplementation is achieved.

This may be due to the fact that DMF has been proven to be a more reactive diester of fumarate (Ruecker *et. al*., 2017, Bergholtz *et al*., 2020), produce a different toxic effect than fumarate inside the cell. In fact, authors like Sullivan *et al.* (2003) and Zheng *et al.* (2015) have reported that this ester is at least ~100-fold more reactive than endogenous fumarate, therefore less selective than fumarate in modifying protein thiols (Merkley *et al.*, 2014). Also, it has been demonstrated in eukaryotes that DMF in micromolar concentrations deprived the cells quickly of gluthatione, a tripeptide composed of glycine, cysteine, and glutamate, and the most abundant and essential intracellular antioxidant (Schmidt & Dringen, 2010). Therefore, it binds to the cysteine

of glutathione to decrease antioxidant capacity and thus enhance endogenous ROS signaling (Schmidt & Dringen, 2010).

In addition, the rapid duplication time of *E. coli* must be considered because it may not be enough for significant intracellular fumarate to accumulate, and thus not cause succination, as cysteine S-succination is a very slow reaction compared to other cysteine reactive electrophiles (Bergholtz *et al*., 2020). On the other hand, the concentrations of how much DMF is added are known, as opposed to not being able to quantify or know the concentrations of intracellular fumarate that accumulates in the Δ*fumABC* mutant, which again, may not be enough.

Furthermore, the effect of supplementation is evident at sub-MIC levels since higher concentrations result in toxicity that impacts growth. Given these points, the effect of DMF could not yet be determined on the basis of growth alone, as it could be pleiotropic.

It is recommended for readings in the Microplate Reader, to measure growth for more than 16 hours, since some strains still showed exponential growth by that time. Similarly, when reading the plates, check for condensation on the lid or loss of volume in the wells to avoid erroneous absorbance data.

Enzymatic activity

Subsequently, as a second approach to validate the succination process in proteins with Fe-S centers, enzyme assays for fumarase and aconitase enzymes were performed to evaluate whether there is a change in their activity upon exposure to fumarate (when deletion of fumarases) or DMF.

a. Fumarase

First, for fumarase activity, the WT strain showed a decrease in its activity when exposed to DMF compared to its exposure to DMSO as a control. The mutant was also exposed to DMSO as a control, as there will be no activity of this enzyme (Figure 15).
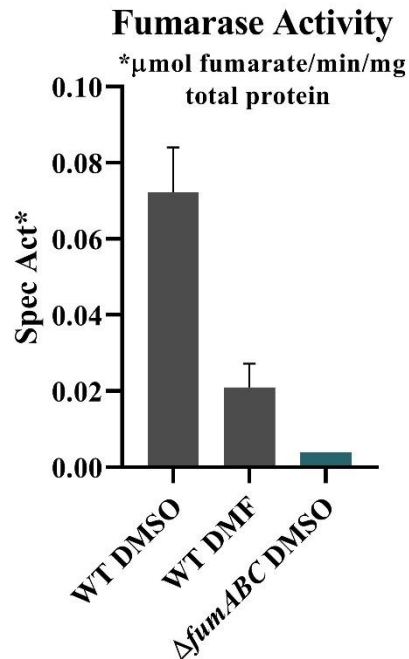
Fumarase Activity

Figure 15. Fumarase activity in WT strain when exposed to DMSO and DMF, and ΔfumABC mutant when exposed to DMSO in M9glycerol medium.

b. Aconitase

Then, if aconitase activity is evaluated in the WT strain, there is also a decrease in its activity when exposed to DMF as compared to when treated with DMSO. However, when evaluating the activity in a Δ*fumABC* triple mutant, aconitase activity is not affected (Figure 16). It can be hypothesized that this could be due to the fact that

fumarate is not producing succination of the cysteines of aconitase, or of other proteins important in the assembly machinery of Fe-S centers, as the DMF is.

Aconitase Activity
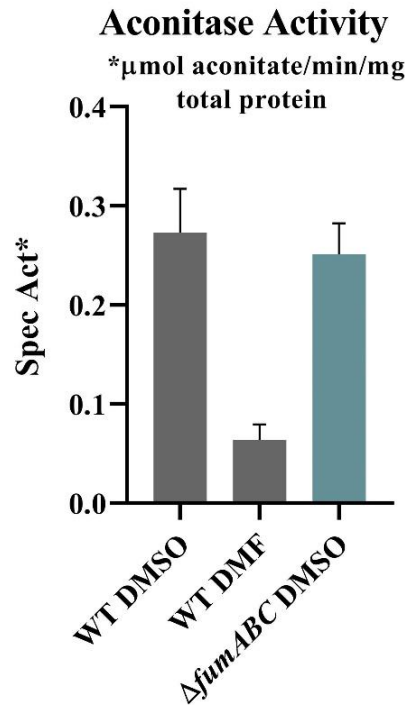
Figure 16. Aconitase activity in WT strain when exposed to DMSO and DMF, and ΔfumABC mutant when exposed to DMSO in M9glycerol medium.

The above not only matches the results obtained from the chemical rescue tests, but can also be compared to what has been studied in eukaryotes, where not all targets are going to be succinated in the same way (Tyrakis *et al*., 2017). For instance, the data provided by proteomics showed that, on the opposite, Succinate dehydrogenase activity is not affected by DMF but reduced when tested in a Δ*fumABC* (Figure 17).

Succinate dehydrogenase Activity

*nmoles NAPDH/min/mg
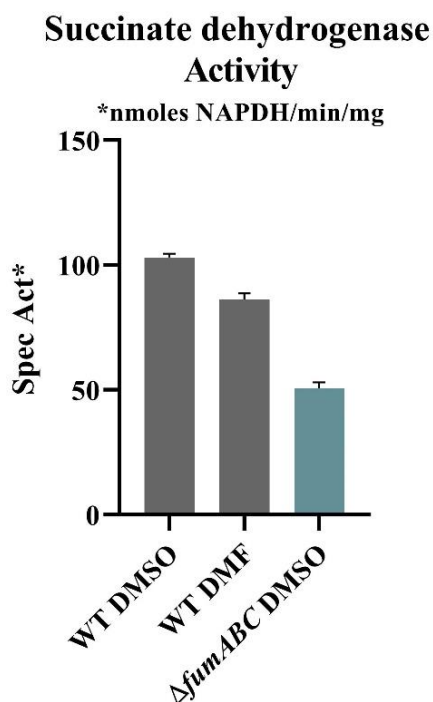
Figure 17. Fumarase activity in WT strain, Δisc and Δsuf mutants when exposed to DMSO and DMF, and ΔfumABC mutant when exposed to DMSO in M9glycerol medium (Data provided by the SAMe laboratory).

The steps in the formation of Fe-S clusters correspond firstly to a scaffold protein in which these clusters are assembled, a cysteine desulfurase providing sulfur in the form of a cysteine bound persulfide (Cys-SSH) and a reductase to reduce the persulfide into sulfide (Gervason *et al*., 2019; Srour *et al*., 2020) In a second step, Fe–S clusters are transferred to recipient apo-proteins with assistance of dedicated chaperones and accessory proteins (Srour *et al*., 2020). Thus, DMF could be causing an effect on cysteines in any of these assembly and transfer steps; for example, by altering the cysteines of the target protein or the ones in the assembly or transfer steps, or even by displacing the Fe-S cluster.

To discern among the possible options, one *in vitro* experiment previously conducted in the SAMe laboratory was considered. Using Fumarase dehydratase as model (FumA), the Fe-S center was first reconstructed in an anaerobic chamber, then exposed

to DMF and MMF and then the enzyme activity was measured; there was no change in enzyme activity compared to the control (DMSO). On the other hand, upon pretreatment with DMF and MMF, and then reconstructing the Fe-S center, the activity was affected (more by DMF than MMF). From the above it can be deduced that DMF could not succinate cysteines in the presence of an Fe-S cluster. Similarly, another *in vitro* assay showed that, by adding DMF to the cys-desulfurase, the Fe-S center can be reconstructed as well.

Another way to determine the site of DMF involvement was to measure the enzymatic activity of fumarase and aconitase, but in Δ*isc* and Δ*suf* mutants, corresponding to the biogenesis machineries of the Fe-s clusters. As mentioned before, Fe-S clusters biogenesis involves three major pathways for their assembly: the ISC (iron-sulphur cluster), SUF (sulphur assimilation) and NIF (nitrogen fixation).

While prokaryotic organisms usually contain either ISC or SUF, some bacterial species such as *Escherichia coli* make use of both systems, yet the proteins of these two systems show differential expression under various environmental and physiological conditions (Tsaousis, 2019; Braymer *et al*., 2021). In undisturbed growth conditions the ISC machinery have the major role in the Fe-S assembly, while in stress conditions such as iron starvation and oxidative environment the assembly is done by the SUF machinery (Braymer *et al*., 2021).

When measuring the fumarase activity of the Δ*isc* mutant, no change was observed if subjected to DMF or DMSO treatment. In contrast, the Δ*suf* mutant decreased its activity upon exposure to DMF compared to the control. This was indicative of the effect on the SUF machinery, which was resistant to DMF while the ISC was not (Figure 18).

47
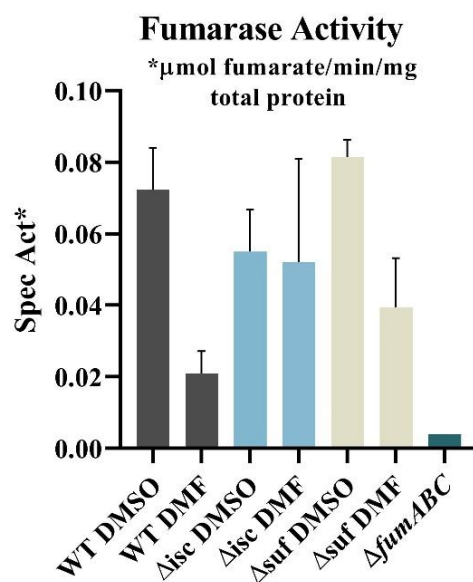
Figure 18. Fumarase activity in WT strain, Δisc and Δsuf mutants when exposed to DMSO and DMF, and ΔfumABC mutant when exposed to DMSO in M9glycerol medium.

When aconitase activity was measured, the opposite effect was observed, since it was in the Δ*isc* mutant whose enzyme activity decreased the most (Figure 19). This could be because the SUF machinery does not recognize aconitase as well as ISC, or even because DMF reacts on aconitase cysteines easier than with fumarase cysteines.
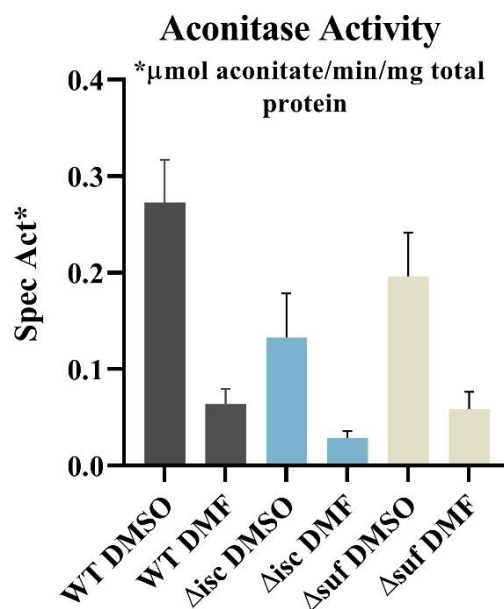
Figure 19.Aconitase activity in WT strain, Δisc and Δsuf mutants when exposed to DMSO and DMF in M9glycerol medium.

From these enzyme assays it was able to validate the succination of TCA cycle proteins containing Fe-S clusters. However, the effect on the activity of these enzymes is not the same if fumarate is accumulated by fumarase deletion as if it is exposed to DMF. Further testing is needed to discriminate exactly where DMF acts. For example, quantitative verification of the succinate cysteines could be performed by liquid chromatography–tandem mass spectrometry (LC–MS/MS) mass spectrometry on the purified protein, and therefore distinguish between the ones from the WT and the mutant, technique already done to distinguish DMF and MMF succination of GAPDH (Kornberg *et al*., 2018).

Also, fumarate itself is not very cell-permeable, which makes it difficult to perform a key mechanistic study, in which hyper S-succination of the proteome is stimulated, and check if protein's activity changes. Even so, the important role of Fe-S centers in protecting cysteines has been proven, and addressing the remaining questions will

improve the understanding of the mechanism by which biogenesis machinery copes with different sources of stress and the mechanism of action of the DMF.

CONCLUSIONS

It was able to validate succination on E. coli mutants by exposure to fumarate analogs DMF and MMF, by looking at final absorbance and growth behaviors. The chemical rescue tests were achieved by adding xanthine (5 µg/mL), adenine (50 µg/mL) and glutamine (5 mM) to the mutants *ΔguaB*, *ΔguaC* and *ΔglnA* respectively. Validation of succination was also achieved for Fe-S cluster proteins by enzymatic assays in vivo.

As for the first approach, supplementation was able to overcome the effect of DMF on the mutants. These results demonstrate that contrary to our first hypothesis, the toxic effect of fumarate accumulation produced by the deletion of fumarases is not equivalent to exposure to DMF in *E. coli*. Furthermore, we observed that there is a different toxic effect between DMF and MMF in the *E. coli* strains.

Likewise, the studied Fe-S proteins decreased their activity when exposed to these treatments. However, Fe-S clusters appear to have a protecting role from succination, thus further tests should follow to determine where succination is occurring, perhaps before insertion of the Fe-S or because of loss of this cofactor by oxidative stress, which would potentially leave the coordinating cysteines exposed to fumarate o fumarate analogs.

Altogether, the results obtained in this study contribute to the evidence that succination is a significant PTM modification and a potential key mechanism linking multiple pathways that may cause dysregulation of cell metabolism in prokaryotes.

REFERENCES

Baba, T., Ara, T., Hasegawa, M., Takai, Y., Okumura, Y., Baba, M., Datsenko, K.A., Tomita, M., Wanner, B.L., Mori, H. (2006) Construction of Escherichia coli K-12 in-frame, single-gene knockout mutants: the Keio collection. *Mol Syst Biol* 2: 2006.0008

Baussier, C., Fakroun, S., Aubert, C., Dubrac, S., Mandin, P., Py, B., & Barras, F. (2020). Making iron-sulfur cluster: Structure, regulation and evolution of the bacterial ISC system. *Advances in Microbial Physiology*, 76, 1–39. https://doi.org/10.1016/bs.ampbs.2020.01.001.

Bergholtz, S. E., Briney, C. A., Najera, S. S., Perez, M., Linehan, W. M., & Meier, J. L. (2020). An Oncometabolite Isomer Rapidly Induces a Pathophysiological Protein Modification. *ACS chemical biology*, *15*(4), 856-861.

Bernatová, S., Samek, O., Pilát, Z., Serý, M., Ježek, J., Jákl, P., Siler, M., Krzyžánek, V., Zemánek, P., Holá, V., Dvořáčková, M., & Růžička, F. (2013). Following the mechanisms of bacteriostatic versus bactericidal action using Raman spectroscopy. *Molecules (Basel, Switzerland)*, *18*(11), 13188–13199. https://doi.org/10.3390/molecules181113188.

Bio-Rad Laboratories Inc. (2005). Quick Start Bradford Protein Assay: Instruction manual.

Blanc, B., Gerez, C., & Ollagnier de Choudens, S. (2015). Assembly of Fe/S proteins in bacterial systems: Biochemistry of the bacterial ISC system. *Biochimica et Biophysica Acta (BBA) - Molecular Cell Research, 1853*(6), 1436-1447. https://doi.org/10.1016/j.bbamcr.2014.12.009

Blewett, M. M., Xie, J., Zaro, B. W., Backus, K. M., Altman, A., Teijaro, J. R., & Cravatt, B. F. (2016). Chemical proteomic map of dimethyl fumarate-sensitive cysteines in primary human T cells. *Science signaling*, *9*(445), rs10.

https://doi.org/10.1126/scisignal.aaf7694

Blount, Z. D. (2015). The unexhausted potential of E. coli. *ELife*, 4, e05826. https://doi.org/10.7554/eLife.05826

Braymer, J. J., Freibert, S. A., Rakwalska-Bange, M., & Lill, R. (2021). Mechanistic concepts of iron-sulfur protein biogenesis in Biology. *Biochimica et Biophysica Acta (BBA)-Molecular Cell Research, 1868*(1), 118863.

Castro, L., Tórtora, V., Mansilla, S., & Radi, R. (2019). Aconitases: Non-redox Iron-Sulfur Proteins Sensitive to Reactive Species. *Accounts of chemical research, 52*(9), 2609–2619. https://doi.org/10.1021/acs.accounts.9b00150.

Ciccarone, F., Di Leo, L., & Ciriolo, M. R. (2019). TCA Cycle Aberrations and Cancer. In P. Boffetta & P. Hainaut (Eds.), Encyclopedia of Cancer (Third Edition) (pp. 429–436). Academic Press. https://doi.org/10.1016/B978-0-12-801238-3.65066-3.

Datsenko, K. A., & Wanner, B. L. (2000). One-step inactivation of chromosomal genes in Escherichia coli K-12 using PCR products. Proceedings of the National Academy of Sciences, 97(12), 6640. https://doi.org/10.1073/pnas.120163297

Derbikov, D. D., Novikov, A. D., Gubanova, T. A., Tarutina, M. G., Gvilava, I. T., Bubnov, D. M., & Yanenko, A. S. (2017). Aspartic Acid Synthesis by Escherichia coli Strains with Deleted Fumarase Genes as Biocatalysts. Applied Biochemistry and Microbiology, 53(9), 859-866. https://doi.org/10.1134/S0003683817090046

Elbing, K. L., & Brent, R. (2019). Recipes and Tools for Culture of Escherichia coli. *Current protocols in molecular biology*, *125*(1), e83. https://doi.org/10.1002/cpmb.83.

Fontecave, M., Py, B., Ollagnier de Choudens, S., & Barras, F. (2008). From iron and cysteine to iron-sulfur clusters: the biogenesis protein machineries. *EcoSal Plus,*

3(1).

Fotie, J. (2018). Inosine 5'-Monophosphate Dehydrogenase (IMPDH) as a Potential Target for the Development of a New Generation of Antiprotozoan Agents. *Mini Reviews in Medicinal Chemistry, 18*(8), 656–671. https://doi.org/10.2174/1389557516666160620065558.

Gerdes, S. Y., Scholle, M. D., Campbell, J. W., Balázsi, G., Ravasz, E., Daugherty, M. D., Somera, A. L., Kyrpides, N. C., Anderson, I., Gelfand, M. S., Bhattacharya, A., Kapatral, V., D'Souza, M., Baev, M. V., Grechkin, Y., Mseeh, F., Fonstein, M. Y., Overbeek, R., Barabási, A. L., Oltvai, Z. N., … Osterman, A. L. (2003). Experimental determination and system level analysis of essential genes in Escherichia coli MG1655. *Journal of bacteriology*, *185*(19), 5673–5684. https://doi.org/10.1128/JB.185.19.5673-5684.2003.

Gervason, S., Larkem, D., Mansour, A. B., Botzanowski, T., Müller, C. S., Pecqueur, L., Le Pavec, G., Delaunay-Moisan, A., Brun, O., Agramunt, J., Grandas, A., Fontecave, M., Schünemann, V., Cianférani, S., Sizun, C., Tolédano, M. B., & D'Autréaux, B. (2019). Physiologically relevant reconstitution of iron-sulfur cluster biosynthesis uncovers persulfide-processing functions of ferredoxin-2 and frataxin. *Nature communications*, *10*(1), 3566. https://doi.org/10.1038/s41467-019-11470-9.

Gillard, G. O., Collette, B., Anderson, J., Chao, J., Scannevin, R. H., Huss, D. J., & Fontenot, J. D. (2015). DMF, but not other fumarates, inhibits NF-κB activity in vitro in an Nrf2-independent manner. *Journal of neuroimmunology*, *283*, 74–85. https://doi.org/10.1016/j.jneuroim.2015.04.006.

Himpsl, S. D., Shea, A. E., Zora, J., Stocki, J. A., Foreman, D., Alteri, C. J., & Mobley, H. L. T. (2020). The oxidative fumarase FumC is a key contributor for E. coli fitness under iron-limitation and during UTI. *PLoS Pathogens, 16*(2), e1008382. https://doi.org/10.1371/journal.ppat.1008382.

Hug, S. M., & Gaut, B. S. (2015). The phenotypic signature of adaptation to thermal stress in Escherichia coli. *BMC Evolutionary Biology*, 15, 177. https://doi.org/10.1186/s12862-015-0457- 3.

Imamura, A., Okada, T., Mase, H., Otani, T., Kobayashi, T., Tamura, M., Kubata, B. K., Inoue, K., Rambo, R. P., Uchiyama, S., Ishii, K., Nishimura, S., & Inui, T. (2020). Allosteric regulation accompanied by oligomeric state changes of Trypanosoma brucei GMP reductase through cystathionine-β-synthase domain. *Nature Communications, 11*(1), 1837. https://doi.org/10.1038/s41467-020-15611-3

Jové, M., Pradas, I., Mota-Martorell, N., Cabré, R., Ayala, V., Ferrer, I., & Pamplona, R. (2020). Succination of Protein Thiols in Human Brain Aging. *Frontiers in Aging Neuroscience*, 12, 52. https://doi.org/10.3389/fnagi.2020.00052.

Joyce, A. R., Reed, J. L., White, A., Edwards, R., Osterman, A., Baba, T., Mori, H., Lesely, S. A., Palsson, B. Ø., & Agarwalla, S. (2006). Experimental and computational assessment of conditionally essential genes in Escherichia coli. *Journal of bacteriology*, *188*(23), 8259–8271. https://doi.org/10.1128/JB.00740-06.

Jung, T., & Mack, M. (2018). Interaction of enzymes of the tricarboxylic acid cycle in Bacillus subtilis and Escherichia coli: A comparative study. *FEMS Microbiology Letters, 365*(8). https://doi.org/10.1093/femsle/fny055.

Keller, J. A., & Simon, L. D. (1987). Isolation and analysis of *Escherichia coli* mutants that allow increased replication of bacteriophage lambda. *Journal of bacteriology, 169(4),* 1585-1592. https://doi.org/10.1128/jb.169.4.1585-1592.1987.

Kessler, A. I., & Gots, J. S. (1985). Regulation of guaC expression in Escherichia coli. *Journal of bacteriology*, *164*(3), 1288–1293.

https://doi.org/10.1128/jb.164.3.1288-1293.1985.

Kornberg, M. D., Bhargava, P., Kim, P. M., Putluri, V., Snowman, A. M., Putluri, N., Calabresi, P. A., & Snyder, S. H. (2018). Dimethyl fumarate targets GAPDH and aerobic glycolysis to modulate immunity. *Science (New York, N.Y.)*, *360*(6387), 449–453. https://doi.org/10.1126/science.aan4665.

Kourakis, S., Timpani, C. A., de Haan, J. B., Gueven, N., Fischer, D., & Rybalka, E. (2020). Dimethyl fumarate and its esters: a drug with broad clinical utility. *Pharmaceuticals*, *13*(10), 306.

Lambden, P. R., & Drabble, W. T. (1973). The gua operon of Escherichia coli K-12: evidence for polarity from guaB to guaA. *Journal of bacteriology*, *115*(3), 992–1002. https://doi.org/10.1128/jb.115.3.992-1002.1973.

Linker, R. A., & Haghikia, A. (2016). Dimethyl fumarate in multiple sclerosis: latest developments, evidence and place in therapy. *Therapeutic advances in chronic disease*, *7*(4), 198–207. https://doi.org/10.1177/2040622316653307.

Margelis, S., D'Souza, C., Small, A. J., Hynes, M. J., Adams, T. H., & Davis, M. A. (2001). Role of glutamine synthetase in nitrogen metabolite repression in Aspergillus nidulans. *Journal of bacteriology*, *183*(20), 5826–5833. https://doi.org/10.1128/JB.183.20.5826-5833.2001.

Millanao, A. R., Mora, A. Y., Saavedra, C. P., Villagra, N. A., Mora, G. C., & Hidalgo, A. A. (2020). Inactivation of Glutamine Synthetase-Coding Gene glnA Increases Susceptibility to Quinolones Through Increasing Outer Membrane Protein F in Salmonella enterica Serovar Typhi. *Frontiers in Microbiology*, 11, 428. https://doi.org/10.3389/fmicb.2020.00428.

Merkley, E. D., Metz, T. O., Smith, R. D., Baynes, J. W., & Frizzell, N. (2014). The succinated proteome. *Mass spectrometry reviews, 33*(2), 98–109. https://doi.org/10.1002/mas.21382.

Moosavi, B., Berry, E. A., Zhu, X.-L., Yang, W.-C., & Yang, G.-F. (2019). The assembly of succinate dehydrogenase: A key enzyme in bioenergetics. *Cellular and Molecular Life Sciences, 76*(20), 4023–4042. https://doi.org/10.1007/s00018-019-03200-7.

Moreno, C., Santos, R. M., Burns, R., & Zhang, W. C. (2020). Succinate Dehydrogenase and Ribonucleic Acid Networks in Cancer and Other Diseases. *Cancers, 12*(11), 3237. https://doi.org/10.3390/cancers12113237.

Piroli, G. G., Manuel, A. M., Walla, M. D., Jepson, M. J., Brock, J. W. C., Rajesh, M. P., Tanis,R. M., Cotham, W. E., & Frizzell, N. (2014). Identification of Protein Succination as a Novel Modification of Tubulin. *The Biochemical Journal, 462*(2), 231–245. https://doi.org/10.1042/BJ20131581.

Ruecker, N., Jansen, R., Trujillo, C., Puckett, S., Jayachandran, P., Piroli, G. G., Frizzell, N., Molina, H., Rhee, K. Y., & Ehrt, S. (2017). Fumarase Deficiency Causes Protein and Metabolite Succination and Intoxicates *Mycobacterium tuberculosis*. *Cell Chemical Biology, 24*(3), 306–315. https://doi.org/10.1016/j.chembiol.2017.01.005.

Sezonov, G., Joseleau-Petit, D., & D'Ari, R. (2007). Escherichia coli physiology in Luria-Bertani broth. *Journal of bacteriology*, *189*(23), 8746–8749. https://doi.org/10.1128/JB.01368-07.

Seta, F. D., Boschi-Muller, S., Vignais, M. L., & Branlant, G. (1997). Characterization of Escherichia coli strains with gapA and gapB genes deleted. *Journal of bacteriology*, *179*(16), 5218-5221.

Shakeel, T., Fatma, Z., & Yazdani, S. S. (2020). *In vivo* Quantification of Alkanes in *Escherichia coli*. *Bio-protocol*, *10*(8), e3593. https://doi.org/10.21769/BioProtoc.3593

Sigma-Aldrich. (n.d.). LB Broth (Miller) Powder microbial growth medium. Millipore

Sigma.https://www.sigmaaldrich.com/catalog/product/sigma/l3522?lang=fr&region=FR.

Silas, Y., Singer, E., Lehming, N., & Pines, O. (2021). A novel combination of Class I fumarase enzymes and a metabolite (alpha-ketoglutarate) signal the DNA damage response in E. coli (p. 2020.08.04.232652). https://doi.org/10.1101/2020.08.04.232652.

Schmidt, M. M., & Dringen, R. (2010). Fumaric acid diesters deprive cultured primary astrocytes rapidly of glutathione. *Neurochemistry international*, *57*(4), 460–467. https://doi.org/10.1016/j.neuint.2010.01.006.

Srour, B., Gervason, S., Monfort, B., & D'Autréaux, B. (2020). Mechanism of iron–sulfur cluster assembly: In the intimacy of iron and sulfur encounter. *Inorganics*, *8*(10), 55.

Sullivan, L. B., Martinez-Garcia, E., Nguyen, H., Mullen, A. R., Dufour, E., Sudarshan, S., & Chandel, N. S. (2013). The proto-oncometabolite fumarate binds glutathione to amplify ROS-dependent signaling. *Molecular cell*, *51*(2), 236-248.

Thomason, L. C., Costantino, N., & Court, D. L. (2007). E. coli genome manipulation by P1 transduction. *Current protocols in molecular biology*, *79*(1), 1-17.

Tyrakis, P. A., Yurkovich, M. E., Sciacovelli, M., Papachristou, E. K., Bridges, H. R., Gaude, E., Schreiner, A., D'Santos, C., Hirst, J., Hernandez-Fernaud, J., Springett, R., Griffiths, J. R., & Frezza, C. (2017). Fumarate Hydratase Loss Causes Combined Respiratory Chain Defects. *Cell Reports, 21*(4), 1036–1047. https://doi.org/10.1016/j.celrep.2017.09.092

Tsaousis, A. D. (2019). On the Origin of Iron/Sulfur Cluster Biosynthesis in Eukaryotes. Frontiers in Microbiology, 10, 2478. https://doi.org/10.3389/fmicb.2019.02478.

Wang, S., Chen, H., Tang, X., Zhang, H., Hao, G., Chen, W., & Chen, Y. Q. (2020). The Role of Glyceraldehyde-3-Phosphate Dehydrogenases in NADPH Supply in the Oleaginous Filamentous Fungus Mortierella alpina. Frontiers in microbiology, 11, 818.

Werner, C., Doenst, T., & Schwarzer, M. (2016). Chapter 4—Metabolic Pathways and Cycles. InM. Schwarzer & T. Doenst (Eds.), The Scientist's Guide to Cardiac Metabolism (pp. 39–55). Academic Press. https://doi.org/10.1016/B978-0-12-802394-5.00004-2.

Westfall, C. S., & Levin, P. A. (2018). Comprehensive analysis of central carbon metabolism illuminates connections between nutrient availability, growth rate, and cell morphology in Escherichia coli. PLoS Genetics, 14(2). https://doi.org/10.1371/journal.pgen.1007205.

Zheng, L., Cardaci, S., Jerby, L., MacKenzie, E. D., Sciacovelli, M., Johnson, T. I., Gaude, E., King, A., Leach, J. D., Edrada-Ebel, R., Hedley, A., Morrice, N. A., Kalna, G., Blyth, K., Ruppin, E., Frezza, C., & Gottlieb, E. (2015). Fumarate induces redox-dependent senescence by modifying glutathione metabolism. *Nature communications*, *6*, 6001. https://doi.org/10.1038/ncomms7001.